www.cad-journal.net
Computer-Aided Design AND APPLICATIONS™

Statistical Shape Modeling for Virtual Bone Reconstruction: An Innovative Approach to Allograft Selection

Alessio Romanelli[1], Michaela Servi[2], Maurizio Scorianz[3], Domenico Andrea Campanacci[4] and Yary Volpe[5]

[1]University of Florence, alessio.romanelli@unifi.it
[2]University of Florence, michaela.servi@unifi.it
[3]AOU Careggi, scorianzm@aou-careggi.toscana.it
[4]AOU Careggi, campanaccid@aou-careggi.toscana.it
[5]University of Florence, yary.volpe@unifi.it

Corresponding author: Yary Volpe, yary.volpe@unifi.it

Abstract. The treatment of malignant bone tumors often involves resection and reconstruction using a prosthesis or donor bone (allograft). Accurate donor-recipient bone matching is crucial, but tumor-related deformities complicate this process. This study explores using a Statistical Shape Model (SSM) to reconstruct the femur's premorbid anatomy for better allograft selection, comparing it with the contralateral mirroring method. The SSM has been developed from 78 healthy femurs obtained after segmentation of post-mortem CT scans. The evaluation of the SSM led to a Generalization of 0.990 mm, a Specificity of 4.622 mm, and a Compactness of 98% with 13 modes of variation. The reconstruction capability of the SSM was assessed on 980 simulated resections. Results showed how the SSM was able to achieve a Chamfer Distance of 1.066 mm and a Hausdorff Distance of 3.229 mm with respect to the original anatomy of the bones. The comparison with the contralateral method showed how this approach offers a promising alternative, particularly when bilateral imaging is not feasible or the contralateral limb is compromised. Furthermore, the retrospective application to a real case of a femur affected by diaphyseal osteosarcoma showed the effectiveness of the proposed SSM in a real case scenario.

Keywords: CAD, Surgical Planning, Statistical Shape Model, Orthopedics, Reconstruction
DOI: https://doi.org/10.14733/cadaps.2026.259-268

1 INTRODUCTION

The treatment of malignant bone tumors often requires the removal of the affected bone segment using planned cutting planes, followed by the implant of a prosthesis [2]. Another widely used approach involves reconstruction using an allograft, which is bone tissue harvested

from a donor [5]. Donor bones are typically supplied by musculoskeletal tissue banks, facilities dedicated to harvesting, preserving, and distributing tissues for transplantation.

Selecting the most appropriate donor is a complex process, where matching the size and shape of the recipient bone plays a vital role in providing good integration. A closer shape matching between donor and recipient can also improve post-operative outcomes, lowering the possibility of fractures or non-unions [13]. Furthermore, allografts taken from the same anatomical site as the affected area exhibit similar mechanical and osteoconductive properties [16]. However, the tumor often alters the recipient bone structure, making it difficult to compare directly with the potential donor bones.

To overcome this challenge, virtual reconstruction of premorbid anatomy is a common approach. The contralateral method, considered the gold standard, consists in the creation of a mirrored 3D model of the healthy contralateral bone, providing an accurate representation of the premorbid anatomy of the affected bone [4, 6, 15].

Nevertheless, this approach is not always a viable option since it requires CT scans of both limbs. Many times, this is not possible since this would expose the patient to an excessive dose of x-ray, and, anyway, it still requires the contralateral to be healthy, which sometimes may not be the case.

Another widely used tool for anatomy reconstruction is Statistical Shape Model (SSM). SSM can learn shape variation from a class of given samples and represent the shape variation using the leading principal components. SSM has been used for reconstruction of the premorbid anatomy of a variety of different bones in the context of many surgical procedures [8, 14, 17].

However, as far as it is known, SSM has never been used for anatomy reconstruction in the context of allograft selection. Therefore, the aim of this work is to develop and evaluate the ability of an SSM to reconstruct the full anatomy of the bone in order to provide a reliable reconstruction that can be used as a comparison to possible donor bones thus improving the allograft selection process. A comparison with the contralateral method is also provided in order to better understand the performance of the proposed approach. This work focused on femurs since they represent a common site for this type of surgery, however, the same approach can be extended to other types of bones.

2 STATISTICAL SHAPE MODEL DEFINITION

The main assumption of a Statistical Shape Model is that all possible shape deformations can be learned from a set of M samples forming an appropriate Training Set $\{\Gamma^1,\Gamma^2,\ldots,\Gamma^M\}$. A complex shape Γ^i can be described as a dense set of landmarks x_k distributed on the surface:

$$\Gamma^i = \; x_k^i \mid x_k^i \in \mathbb{R}^3, k = 1,\ldots,N_i$$

Where N_i is the number of points used to describe the shape i, and x_k contains the 3 Cartesian coordinates of the k-th point.

The crucial assumption is that the landmark points are in correspondence among the samples. This means that the k-th landmark of two shapes Γ^i and Γ^j represents the same anatomical point of the shape. Finding a meaningful correspondence between shapes is one of the critical tasks of statistical shape analysis. Once it is established, all shapes can be described with the same number of points N. Therefore, by defining each shape Γ^i as a vector $\vec{x}_i \in \mathbb{R}^{3N}$ consisting of the stacked x,y,z components of each point, the shape variations can be modeled using a normal distribution, where the mean $\bar{x}$ and covariance matrix L are estimated as follows:

$$\bar{x} = \frac{1}{M}\sum_{i=1}^{M}\vec{x}_i \tag{1}$$

$$L = \frac{1}{M-1}\sum_{i=1}^{M}\left(\vec{x}_i - \bar{x}\right)\left(\vec{x}_i - \bar{x}\right)^T \tag{2}$$

However, since the number of landmark points describing the samples is usually quite large, a high amount of data is necessary to represent the covariance matrix L explicitly. Fortunately, as it is determined completely by the samples, it has at most rank M and can therefore be represented using M basis vectors. This is achieved by performing a Principal Component Analysis [7], thus leading to the following definition of SSM:

$$x = \bar{x} + \sum_{m=1}^{c}\alpha_m\sqrt{\lambda_m}\varphi_m \tag{3}$$

where λ_m and φ_m are, respectively, the eigenvalues and eigenvectors of matrix L, α_m follows a normal distribution with a mean of 0 and a standard deviation of 1, and c represents the number of significant eigenvalues. The number c is defined so that the accumulated variance reaches a certain ratio of the total variance, usually between 0.9 and 0.98 (in this work, 0.98 is used). Equation 3 allows for an efficient, parametric representation of the distribution.

Although the entire process appears simple, determining the correspondences is a challenging step since the quality of the SSM itself is heavily influenced by the established correspondences. The most widely used methods for this task rely on the Iterative Closest Point (ICP) algorithm [1] or the Coherent Point Drift (CPD) algorithm [11]. In this work, the algorithm described in [9] is used to establish the correspondences between samples of the training set.

For this study, the training set consisted of 78 healthy right femurs (42 males, 36 females, mean age: 29.4 years). The 3D models of the femurs were obtained by segmentation, using the software Materialise Mimics 26 [10], of post-mortem Computed Tomography Images obtained from the New Mexico Decedent Image Database [3]. In order to reduce computational load, the 3D models were then decimated to 20’000 points. The 3D models were first translated to align their centroid with the origin of the Global Reference System. After that, a reference shape was chosen randomly from the training set, and all other femurs were aligned to the reference using a rigid ICP algorithm in order to remove relative rotation between the models. Then the algorithm described in [9] was used to establish correspondences. At this point, the mean shape and the covariance matrix could then be computed through Equations 1 and 2. By performing Principal Component Analysis, the SSM was defined through Equation 3.

3 STATISTICAL SHAPE MODEL EVALUATION

The most widely used approach for assessing the quality of an SSM is based on three key properties: Generalization, Specificity, and Compactness [8].

The first property, Generalization (G), measures how well the SSM can replicate a given shape. It is typically assessed through a series of leave-one-out tests on the training set, by computing the distance between the omitted shape Γ^i and its closest match $\Gamma^i_*(c)$ generated by the reduced SSM. The Generalization is given as a function of the number c of the significant eigenvalues used to define the parametric model:

$$G(c) = \frac{1}{M}\sum_{i=1}^{M} D\ \ \Gamma_*^i(c), \Gamma^i \tag{4}$$

Lower G values correspond to better-performing SSMs. The metric D is used to quantify the distance between shapes. Following the approach in [8], this study uses the Symmetric Mean (SM) distance as metric D.

The second metric is Specificity (S), which evaluates the ability of the model to produce new shapes that are consistent with the family of shapes encoded in the model. This is evaluated by generating random parameter sets of α and calculating the average distance between each corresponding generated shape $\Gamma_{**}^k(c)$ and its nearest match in the training set, over a large number of iterations (t). As Generalization, Specificity is given as a function of the number of significant eigenvalues c:

$$S(c) = \frac{1}{t}\sum_{k=1}^{t} \min_{i=1,\ldots,M} D\ \ \Gamma_{**}^k(c), \Gamma^i \tag{5}$$

where the metric D used for Specificity is the Mean Absolute Distance between corresponding points to make the measurement robust and independent from the number of landmarks [8].

Interestingly, $S(c)$ tends to worsen as c increases. While this may seem counterintuitive, it can be explained by noticing that greater variability allows the SSM to elude the training set members more easily.

The last metric, Compactness (C), represents the cumulative variance of the model as determined by principal component analysis (PCA). In this work C was normalized with respect to the total variance:

$$C(c) = \frac{\sum_{i=1}^{c} \lambda_i}{\sum_{j=1}^{M-1} \lambda_j} \tag{6}$$

A compact model, characterized by a low c value, requires fewer parameters to encode greater variability within the training set. In contrast to the first two measures, higher C values correspond to better SSMs.

Generalization, Specificity, and Compactness for the SSM constructed in this work are reported in Figure. As can be seen from Figure 1c the first mode of variation accounts for 90.7% of the total variance of the model. Compactness grows quickly reaching the value of 98% for $c = 13$, indicating that a compact model can represent the great majority of the possible shapes encoded in the model. Furthermore from Figure 1a and Fig.1b it can be noted how the curves of Generalization and Specificity flatten for $c > 10$ meaning that $c = 13$ is a good choice to balance the ability to replicate a given shape ($G = 0.990\ mm$ for $c = 13$) and the ability to generate new shapes consistent with the family of shapes encoded in the model ($S = 4.622\ mm$ for $c = 13$).

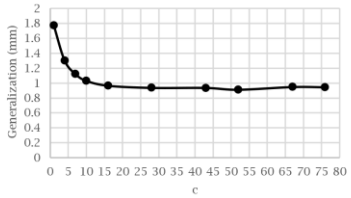

(a)

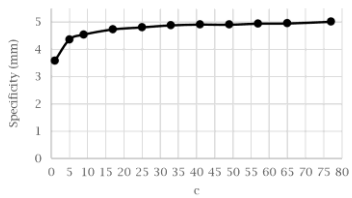

(b)

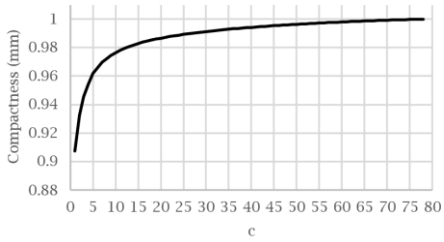

(c)

Figure 1: (a) Generalization, (b) Specificity, (c) Compactness as a function of the number of modes of variation c.

4 RECONSTRUCTION OF MISSING ANATOMY

After building and evaluating the SSM, its ability to infer the complete shape of a femur from a partial one was tested. A dataset of 49 femurs was chosen randomly from the 78 femurs composing the training set of the SSM.

Through the software Geomagic Design X [12], 20 different configurations of resection were generated and replicated on each of the 49 cases in the dataset such that a total of 980 partial femurs representing simulated clinical cases, were obtained.

A series of leave-one-out tests were performed, meaning that for each of the 49 cases, an SSM was built using the remaining 77 femurs, then the reduced SSM was used to infer the full shape of the femur for the 20 different resections using $c = 13$. Since our aim is to evaluate the ability of the SSM in reconstructing only the missing part of the bone, the corresponding partial femur was aligned to the SSM inferred full bone using the ICP algorithm [1]. Then following the contour of resection of the partial femur, the SSM full bone was cut in the same way in order to extract the missing part of the bone. Some examples of reconstruction are reported in Figure 2.

To better understand the performance of the built SSM in the task of reconstructing the missing anatomy, the gold standard technique of leveraging the contralateral bone was also performed. Specifically, for each of the 49 right femurs, the corresponding left femur (which from now on will be referenced as "contralateral") was segmented from the same CT images, then the 3D model was resampled to about 20'000 points and, finally, mirrored (the axis of mirroring can be any, since it influences only the position and orientation of the resulting mirrored 3D model). To extract the missing part of the bone, the same procedure described above for the SSM was followed.

To quantitatively evaluate the similarity between the reconstructions generated by the SSM (or the contralateral) and the real anatomy of the bone, Chamfer Distance (CD) and Hausdorff Distance (HD) were used; CD and HD between two-point clouds P_1 and P_2 can be defined as:

$$CD\ P_1,P_2 = \frac{1}{2}\left(\frac{1}{|P_1|}\sum_{x\in P_1}\left\|x-\overline{y}\right\|_2 + \frac{1}{|P_2|}\sum_{y\in P_2}\left\|y-\overline{x}\right\|_2\right) \tag{7}$$

$$HD\ P_1,P_2 = \frac{1}{2}\left(\max_{x\in P_1}\left\|x-\overline{y}\right\|_2 + \max_{y\in P_2}\left\|y-\overline{x}\right\|_2\right) \tag{8}$$

where $\overline{y} = \left\{ y \in P_2 \mid d(x,y) = \min_{y \in P_2} \left\| x - y \right\|_2 \right\}$ (and similarly for $\overline{x}$), while $|P_1|$ and $|P_2|$ represent the number of points of each point cloud. Thus CD can be intended as the mean distance between the two point clouds, while the HD as the maximum distance.

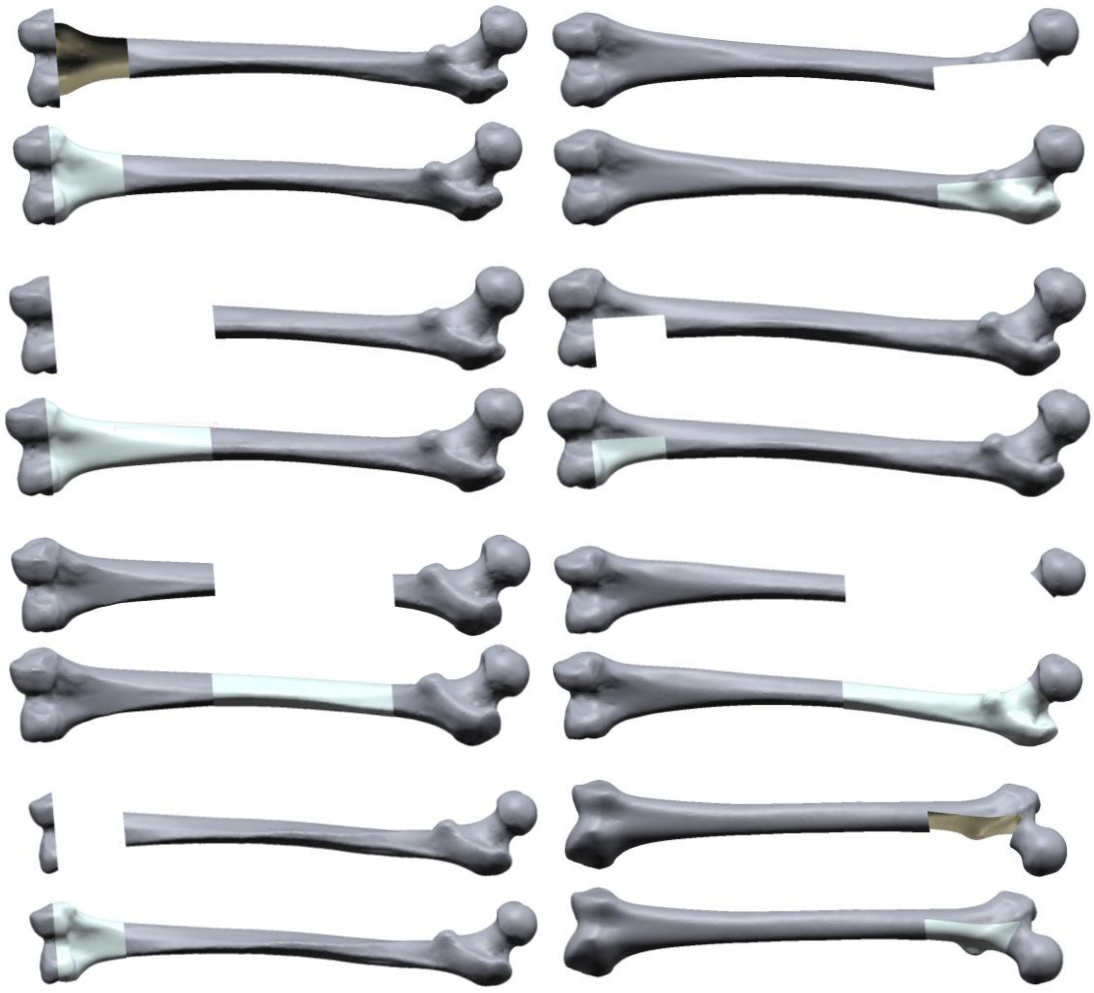

Figure 2: Examples of reconstruction using 13 modes of variation.

In Figure 3 the mean and standard deviation of HD and CD, calculated across all 980 cases, for both SSM and Contralateral method, are reported. As can be seen, the constructed SSM was able to reconstruct the missing anatomy with a mean CD of 1.066 mm and, as expected, is outperformed by the gold standard contralateral method which was able to infer the missing part of the bone with a mean CD of 0.759 mm. However, these results show that, despite not reaching the performance of the contralateral method, the CD and HD values of the SSM and Contralateral method are respectively only 0.3 mm and 1.3 mm apart on average and thus the SSM stands as a valid solution to reduce the dose of radiation on the patient or in cases where even the contralateral is compromised.

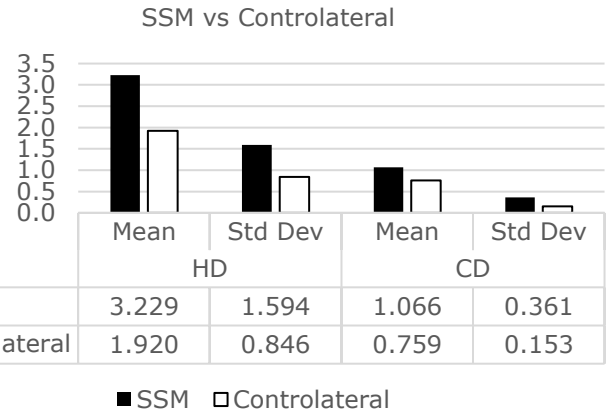

	HD		CD	
	Mean	Std Dev	Mean	Std Dev
SSM	3.229	1.594	1.066	0.361
Controlateral	1.920	0.846	0.759	0.153

Figure 3: Chamfer Distance and Hausdorff Distance mean and standard deviation across all 980 reconstructions.

4.1 Case Study

In order to show the performance of the proposed SSM, retrospective application to a real case of femur affected by tumor, which underwent surgery at the University Hospital Careggi of Florence, is presented. Specifically, as can be seen in Figure 4: Retrospective study of a case of femoral diaphyseal osteosarcoma: a) on the left the 3D models of the femur and the tumor, on the right the partial femur after resection of the affected part; b) on the left, in white, the missing part reconstructed by the SSM, on the right, in blue, the reconstructed part with the contralateral method. Figure a, the case involved a femoral diaphyseal osteosarcoma.

After removing the part of the bone affected by the tumor using the cutting planes identified by the surgeon, the full bone of the femur was inferred leveraging the built SSM. As shown, the segmented femur includes only the diaphyseal and distal regions, as the CT scan was acquired excluding the hip, which was unaffected by the tumor and thus spared from unnecessary radiation exposure. However, despite the limited information present in the partial femur, the SSM was still able to infer the full shape of the bone consistently (see Figure b).

To isolate only the missing portion of the partial bone, it was aligned with the SSM-inferred full bone using the ICP algorithm. Once the registration is executed the cutting planes can be used to cut the SSM bone and extract the missing part.

Since for this specific case a bilateral CT was available, the contralateral method was also used. The resulting reconstructed parts of the SSM and contralateral method are shown in Figure b. Since no ground truth, i.e. real anatomy of the pathological bone, is available for a real case, a quantitative evaluation is not possible. However, as reported in Figure b, Chamfer Distance and Hausdorff Distance between the SSM and contralateral method reconstructed parts (white and blue in Figure b respectively) were computed. In the light of subsequent process of allograft selection, which consists in comparing the reconstructed anatomy with every donor, the CD and HD values obtained can be considered acceptable since it will be nearly impossible to find a donor that matches perfectly the reconstructed anatomy.

5 CONCLUSIONS

The reconstruction of the premorbid anatomy of the bone is a fundamental part of allograft selection since a reference shape is needed to select the best shape-matching donor. To this regard, the contralateral method represents the gold standard technique; however a bilateral

CT may not always be available. For this reason, in this work, a Statistical Shape Model of the full femur was built from 78 healthy right femurs.

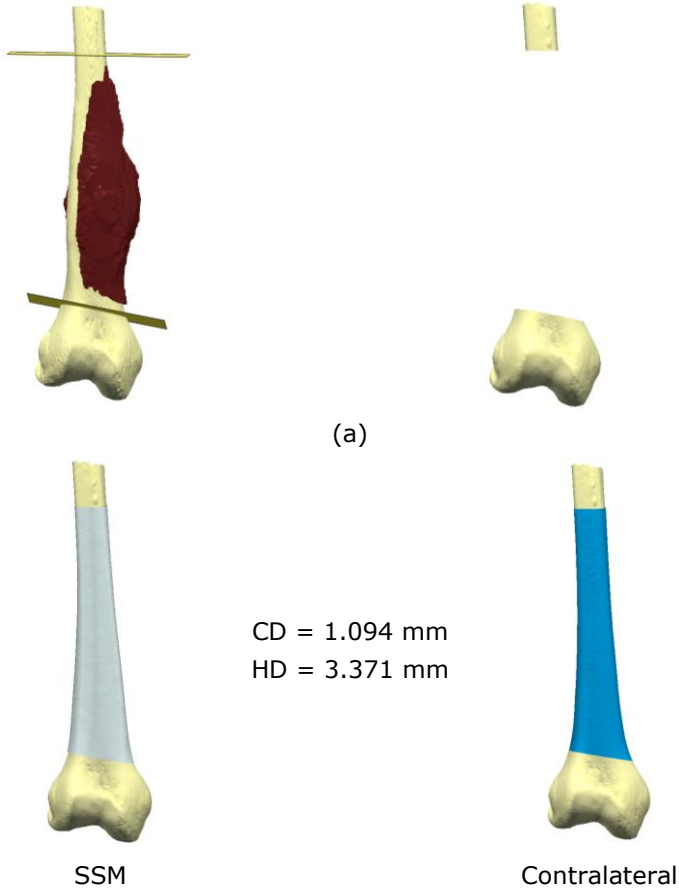

Figure 4: Retrospective study of a case of femoral diaphyseal osteosarcoma: a) on the left the 3D models of the femur and the tumor, on the right the partial femur after resection of the affected part; b) on the left, in white, the missing part reconstructed by the SSM, on the right, in blue, the reconstructed part with the contralateral method.

Evaluation of the SSM showed how a compact model with only 13 modes of variation was able to achieve a Generalization of 0.990 mm and a Specificity of 4.622 mm. The ability of the SSM in reconstructing the missing part of the bone was vastly tested, upon nearly 1000 simulated cases, showing a Chamfer Distance of 1.066 mm and Hausdorff Distance of 3.229 mm with respect to the real anatomy of the bone. A comparison with the contralateral method was performed showing how, despite being outperformed, the SSM still stands out as a great alternative, being able to infer the premorbid anatomy with a Chamfer Distance only 0.3 mm worse on average than the contralateral method. Furthermore, the case study presented showed how the proposed method can be easily and effectively used in a real case scenario.

Still some limitations emerge as a dataset of 3D models of healthy bones is necessary for the construction of the SSM, whose realization requires manual and time-expensive work in the process of segmentation of CT or MRI images. To this regard future work should focus on leveraging Deep Neural Networks to automatically segment medical images.

Alessio Romanelli, https://orcid.org/0009-0009-2941-6740
Michaela Servi, https://orcid.org/0000-0002-4071-6615
Maurizio Scorianz, https://orcid.org/0000-0002-7164-065X
Domenico Andrea Campanacci, https://orcid.org/0000-0002-3912-3943
Yary Volpe, https://orcid.org/0000-0002-5668-1912

REFERENCES

[1] Besl, P.-J; McKay, N.-D: A Method for Registration of 3-D Shapes, IEEE Transactions on Pattern Analysis and Machine Intelligence, 14(2), 1992, 239–256. https://doi.org/10.1109/34.121791
[2] Calderón, S.-A.-L.; Kuechle, J.; Raskin, K.-A., Hornicek, F.-J.: Lower Extremity Megaprostheses in Orthopaedic Oncology, The Journal of the American Academy Orthopaedic Surgeons, 26(12), 2018 e249–e257. https://doi.org/10.5435/JAAOS-D-16-00218
[3] Edgar, H.-J.-H.; Daneshvari, Berry S.; Moes, E.; Adolphi, N.; Bridges, P.; Nolte, K.: New Mexico Decedent Image Database, Office of the Medical Investigator, University of New Mexico, 2020.
[4] Ferràs-Tarragó, J.; Sanchis-Alfonso, V.; Ramírez-Fuentes, C.; Roselló-Añón, A.; Baixauli-García, F.: A 3D-CT Analysis of Femoral Symmetry—Surgical Implications, Journal of Clinical Medicine 9(11), 2020, 3546. https://doi.org/10.3390/jcm9113546
[5] Houdek, M.-T.; Sullivan, M.-H.; Broida, S.-E.; Barlow, J.-D.; Morrey, M.-E.; Moran, S.-L.; Sanchez-Sotelo, J.: Proximal Humerus Reconstruction for Bone Sarcomas: A Critical Analysis, JBJS Reviews, 12(3), 2024. https://doi.org/10.2106/JBJS.RVW.23.00217
[6] Jacquet, C.; Laumonerie, P.; LiArno, S.; Faizan, A.; Sharma, A.; Dagneaux, L.; Ollivier, M.: Contralateral preoperative templating of lower limbs' mechanical angles is a reasonable option, Knee Surgery, Sports Traumatology, Arthroscopy, 28(5), 2020, 1445–1451. https://doi.org/10.1007/s00167-019-05524-0
[7] Joliffe, I.-T.: Principal Component Analysis, Springer New York, New York, NY, 2002. https://doi.org/10.1007/b98835
[8] Marzola, A.; McGreevy, K.-S.; Mussa, F.; Volpe, Y.; Governi, L.: HyM3D: A hybrid method for the automatic 3D reconstruction of a defective cranial vault, Computer Methods and Programs in Biomedicine, 2023, 234. https://doi.org/10.1016/j.cmpb.2023.107516
[9] Marzola, A.; Servi, M.; Volpe, Y.: A Reliable Procedure for the Construction of a Statistical Shape Model of the Cranial Vault, Lecture Notes in Mechanical Engineering, 2020, 788–800. https://doi.org/10.1007/978-3-030-31154-4_67
[10] Materialise Mimics 26, https://www.materialise.com/en/healthcare/mimics-innovation-suite/26, Materialise, 2023.
[11] Myronenko, A.; Song, X.: Point set registration: coherent point drift, IEEE Transactions on Pattern Analysis Machine Intelligence, 2010, 32(10), 2262–2275. https://doi.org/10.1109/TPAMI.2010.46
[12] Geomagic Design X 2024.1, https://oqton.com/geomagic-designx, Oqton, 2024.
[13] Pala, E.; Canapeti, J.; Trovarelli, G.; Angelini, A.; Ruggieri, P.: Is still effective massive allograft reconstruction in parosteal osteosarcoma of the distal femur? Review of the literature and advantages of newer technologies, Journal of Orthopaedic Surgery and Research, 2024, 19(1), 395. https://doi.org/10.1186/s13018-024-04880-z
[14] Salhi, A.; Burdin, V.; Boutillon, A.; Brochard, S.; Mutsvangwa, T.; Borotikar, B.: Statistical Shape Modeling Approach to Predict Missing Scapular Bone, Annals of Biomedical Engineering, 2020, 48(1), 367–379. https://doi.org/10.1007/s10439-019-02354-6
[15] Sparks, C.-A.; Decker, S.-J.; Ford J.-M.: Three-Dimensional Morphological Analysis of Sex, Age, and Symmetry of Proximal Femurs from Computed Tomography: Application

to Total Hip Arthroplasty, Clinical Anatomy, 2020, 33(5), 731–738. https://doi.org/10.1002/ca.23496

[16] Wu, Z.; Fu, J.; Wang, Z.; Li, X.; Li, J.; Pei, Y.; Pei, G.; Li, D.; Guo, Z.; Fan, H.: Three-dimensional virtual bone bank system for selecting massive bone allograft in orthopaedic oncology, International Orthopaedics, 2015, 39(6), 1151–1158. https://doi.org/10.1007/s00264-015-2719-5

[17] Zhou, C.; Cha, T.; Peng, Y.; Bedair, H.; Li, G.: 3D Geometric Shape Reconstruction for Revision TKA and UKA Knees Using Gaussian Process Regression Annals of Biomedical Engineering, 2021, 49(12), 3685–3697. https://doi.org/10.1007/s10439-021-02871-3